Targeting translocator protein protects against myocardial ischemia/reperfusion injury by alleviating mitochondrial dysfunction

CHENGHAO WEN[1*], YUNFEI JIANG[1*], WEN CHEN[1], YUEYUE XU[1], GANYI CHEN[1], QIANG ZHOU[1], QUAN LIU[2], HONGWEI JIANG[1], YAFENG LIU[1], XU CAO[1], YIWEI YAO[1], RUOYU ZHANG[1], ZHIBING QIU[1] and SHENGCHEN LIU[1]

[1]Department of Thoracic and Cardiovascular Surgery, Nanjing First Hospital, Nanjing Medical University, Nanjing, Jiangsu 210006, P.R. China; [2]Department of Thoracic and Cardiovascular Surgery, Nanjing First Hospital, Southeast University, Nanjing, Jiangsu 210006, P.R. China

Received February 1, 2024; Accepted June 11, 2024

DOI: 10.3892/etm.2024.12638

Abstract. Ischemic heart disease (IHD) remains a leading cause of mortalities worldwide, necessitating timely reperfusion to reduce acute mortality. Paradoxically, reperfusion can induce myocardial ischemia/reperfusion (I/R) injury, which is primarily characterized by mitochondrial dysfunction. Translocator protein (TSPO) participates in multiple cellular events; however, its role in IHD, especially in the process of myocardial I/R injury, has not been well determined. The aim of the present study was to investigate the functional role of TSPO in myocardial I/R injury and dissect the concomitant cellular events involved. This study utilized small interfering RNA (siRNA) technology to knock down TSPO expression. The I/R process was simulated using an anoxia/reoxygenation (A/R) model. The role of TSPO in H9c2 cardiomyocytes was assessed using various techniques, such as Western blotting, Flow cytometry, Reverse transcription-quantitative PCR (RT-qPCR), Immunofluorescence, Co-immunoprecipitation (co-IP) and similar methods. It was found that A/R markedly upregulated the expression of TSPO in cardiomyocytes. Inhibition of TSPO improved myocardial cell apoptosis and damage following A/R stimulation. Additionally, targeting TSPO alleviated mitochondrial damage, reduced mitochondrial ROS release and enhanced ATP synthesis following A/R stimulation. It was further confirmed that A/R stimulation induced a significant increase in the expression of pivotal markers [phosporylated-PKR-like ER kinase (PERK)/PERK, activating transcription factor 6 (ATF6) and inositol-requiring enzyme 1] involved in the adaptive unfolded protein response, which is accompanied by downstream signaling during endoplasmic reticulum (ER) stress. Notably, *TSPO* knockdown increased the expression of the aforementioned markers and, subsequently, TSPO was confirmed to interact with ATF6, suggesting that TSPO might play a role in ER stress during myocardial I/R injury. Finally, inhibition of TSPO upregulated mitophagy, as indicated by further decreases in P62 and increases in Parkin and PINK1 levels following A/R stimulation. Together, the results suggest that TSPO plays a multifaceted role in myocardial I/R injury. Understanding TSPO-induced cellular responses could inform targeted therapeutic strategies for patients with IHD.

Introduction

Ischemic heart disease (IHD) is a major cause of global mortality and is a substantial burden on individuals and healthcare systems (1). Conventional clinical strategies for treating acute myocardial infarction include coronary artery intervention and other reperfusion therapies to minimize the ischemic time (2). Although timely reperfusion significantly reduces acute mortality in patients with ST-segment elevation myocardial infarction (3), partial cell damage occurs during the reperfusion phase, known as ischemia/reperfusion (I/R) injury, which has garnered significant attention (4). The mechanisms underlying myocardial I/R injury are intricate, involving multiple cellular events such as oxidative stress, intracellular calcium overload cell apoptosis (5). Notably, the excess generation of reactive oxygen species (ROS) by mitochondria during I/R is a crucial trigger of the aforementioned cellular events (6). The mitochondrial electron transport chain (ETC), which is damaged during ischemia, is associated with mitochondrial dysfunction and excessive production of

Correspondence to: Professor Zhibing Qiu or Dr Shengchen Liu, Department of Thoracic and Cardiovascular Surgery, Nanjing First Hospital, Nanjing Medical University, 68 Changle Road, Nanjing, Jiangsu 210006, P.R. China
E-mail: qiuzhibing2009@163.com
E-mail: shengchen_liu@163.com

*Contributed equally

Key words: myocardial ischemia/reperfusion injury, translocator protein, mitochondrial dysfunction, endoplasmic reticulum stress, mitophagy

ROS. During reperfusion, damaged mitochondria undergo further injury, activating programmed cell death pathways in cardiomyocytes (7,8).

Translocator protein (TSPO) is an 18 kDa protein located on the outer mitochondrial membrane (OMM) (9). It is found in the cardiovascular system and is associated with both myocardial injury and protection (10,11). TSPO was first discovered in human cortical tissues (12), and its primary function had been revealed to involve the transport of cholesterol from the OMM to the inner mitochondrial membrane (13). TSPO actively participates in ATP and ROS production in mitochondria and triggers cell apoptosis (14). Gatliff *et al* (15) and Meng *et al* (16) reported that TSPO overexpression reduces mitochondrial coupling and promotes the overproduction of ROS in canine mammary gland epithelia. TSPO has also been shown to inhibit mitophagy, preventing the clearance of damaged mitochondria (17). It is apparent that a severe consequence of myocardial I/R is oxidative injury, which leads to mitochondrial dysfunction (18). Based on the aforementioned observations, it has been hypothesized that TSPO may play a vital role in myocardial I/R injury by regulating mitochondrial homeostasis.

In the present study, an *in vitro* model of anoxia/reoxygenation (A/R) injury was established using H9c2 cardiomyocytes to simulate myocardial I/R injury. It was observed that TSPO expression was significantly increased following A/R injury. This study aims to explore the function and mechanisms of TSPO in myocardial ischemia-reperfusion injury. Taken together, targeting TSPO could be a potential strategy for alleviating myocardial I/R injury.

Materials and methods

H9c2 cardiomyocyte culture. H9c2 cardiomyocytes were cultured following the methodology described by Pooja *et al* (19). Briefly, H9c2 cardiomyocytes were obtained from The Cell Bank of Type Culture Collection of The Chinese Academy of Sciences and cultured in DMEM supplemented with 10% FBS (Gibco; Thermo Fisher Scientific, Inc.) and 1% penicillin/streptomycin solution (Gibco; Thermo Fisher Scientific, Inc.). The cells were maintained in a humidified incubator at 37˚C supplied with 5% CO_2 air (Thermo Fisher Scientific, Inc.), and the culture medium was replaced every 2 days.

RNA interference. In the present study, three small interfering (si)RNA constructs were obtained from Shanghai GenePharma Biotechnology Co., Ltd. and transfected using siRNA-Mate (Shanghai GenePharma Biotechnology Co., Ltd.). After confirmation of knockdown using western blotting, the si-RNA3-TSPO sequence, which exhibited the best knockdown efficiency, was selected for further experiments. Briefly, for si-TSPO and A/R-si-TSPO group, 3 μl siRNA and 4 μl siRNA-mate were diluted in 200 μl Opti-MEM (Gibco; Thermo Fisher Scientific, Inc.). For si-NC and A/R-si-NC group, 3 μl siRNA-negative control and 4 μl siRNA-mate were diluted in 200 μl Opti-MEM (Gibco; Thermo Fisher Scientific, Inc.), incubated at room temperature for 5 min, mixed thoroughly and incubated for 15 min. H9c2 cardiomyocytes were treated with the mixture and incubated at 37˚C for 72 h. After incubation, cells in the si-TSPO group and si-NC group were replaced with complete culture medium and placed in a culture incubator for cultivation. Cells in the A/R-si-TSPO group and A/R-si-NC group were immediately subjected to anoxia/reoxygenation stimulation and were then used together for subsequent experiments. The sequences of these siRNA fragments are shown in Table I, and the knockdown efficiency is shown in Fig. S1.

Establishment of the in vitro anoxia/reoxygenation (A/R) model. The A/R model was established following a procedure described by Tong *et al* (20) with modifications. Briefly, cells in the A/R group were subjected to anoxic treatment for 3 h in glucose-free DMEM (cat. no. 11966-025; Gibco; Thermo Fisher Scientific, Inc.) under oxygen-depleted conditions. For Hypoxia, the cells were placed in an anoxic chamber with a deoxygenation bag (AnaeroPack™, Mitsubishi Gas Chemical Company, Inc.) and then reoxygenated for 2 h with complete medium in a humidified incubator at 37˚C supplied with 5% CO_2 air. After 2 h of reoxygenation treatment, the cells were harvested and the medium was collected immediately for subsequent analysis.

Flow cytometry. According to the instructions of the reagent kit (cat. no. WLA001a; Wanleibio Co., Ltd.), flow cytometry was used to detect cell apoptosis. After specific treatment, the cells were digested with 0.25% trypsin-EDTA (1x) (Gibco; Thermo Fisher Scientific, Inc.) and collected by centrifugation at 100 x g for 5 min at room temperature. Subsequently, the cells were resuspended in 500 μl binding buffer (cat. no. WLA001a; Wanleibio Co., Ltd.). Propidium iodide and annexin V conjugated with fluorescein isothiocyanate (cat. no. WLA001a; Wanleibio Co., Ltd.) were added to the cells and incubated in the dark at room temperature for 15 min. A flow cytometer (model no. B73613, DxFLEX; Beckman Coulter, Inc.) was then used for analysis, The flow cytometry results were analyzed using FlowJo™ Software (version 10.8.1; BD Life Sciences); three independent experiments were performed, and samples were assessed in triplicate.

Detection of mitochondrial membrane potential. A Mitochondrial Membrane Potential Assay Kit with JC-1 (cat. no. C2006; Beyotime Institute of Biotechnology) was used according to the manufacturer's protocol. JC-1 working solution was added to H9c2 cells at a dilution of 1:1,000, and the cells were incubated at 37˚C for 20 min. Cells were subsequently washed three times with the JC-1 buffer and then observed using a fluorescence microscope.

ROS staining. Intracellular ROS levels and mitochondrial ROS (mtROS) generation were detected using DCFH-DA (cat. no. S0033S; Beyotime Institute of Biotechnology) and MitoSOX, respectively (cat. no. M36008; Invitrogen; Thermo Fisher Scientific, Inc.). Cells on slides were treated with 10 μM DCFH-DA for 20 min at 37˚C in the dark in a humid chamber. Subsequently, they were treated with MitoSOX red mitochondrial superoxide indicator at a dilution of 1:1,000 in a dark and humid room at 37˚C for 10 min. The number of ROS-positive cells in four randomly selected fields of view was observed using a fluorescence microscope.

Table I. Sequences of three pairs of TSPO gene interference fragments and negative control.

siRNA	Sequence (5'-3')
siRNA1-TSPO-sense	GCUCCUACAUAAUCUGGAATT
siRNA1-TSPO-anti-sense	UUCCAGAUUAUGUAGGAGCTT
siRNA2-TSPO-sense	CCAUGCUCAACUACUAUGUTT
siRNA2-TSPO-anti-sense	ACAUAGUAGUUGAGCAUGGTT
siRNA3-TSPO-sense	GGGCCUUUAAAGCUAAAUATT
siRNA3-TSPO-anti-sense	UAUUUAGCUUUAAAGGCCCTT
siRNA-negative control-sense	UUCUCCGAACGUGUCACGUTT
siRNA-negative control-anti-sense	ACGUGACACGUUCGGAGAATT

siRNA, small interfering RNA; TSPO, translocator protein.

Cell viability assay. After specific treatments, the cells were digested as above, counted, and then transferred to a 96-well plate. A total of 10 μl CCK8 reagent (cat. no. K1018; APExBIO Technology LLC) was added to each well, and the plate was incubated at 37˚C for 1 h. The enzymatic activity was then measured using a microplate reader at a wavelength of 450 nm.

Determination of LDH, SOD, MDA, and ATP levels. For determination of lactate dehydrogenase (LDH) levels, 0.1 ml culture medium was collected from each experimental group immediately following A/R treatment and analyzed according to the manufacturer's protocol (cat. no. A020-2; Nanjing Jiancheng Bioengineering Institute). Subsequently, the cells were washed twice with PBS and, after complete removal of PBS, lysed with RIPA lysis buffer (cat. no. P0013D; Beyotime Institute of Biotechnology). The lysates were then incubated in an ice bath for 10 min, followed by centrifugation at 13,400 g for an additional 10 min at 4˚C to obtain the supernatant. The resulting supernatant was used to measure the levels of superoxide dismutase (SOD; cat. no. A001-3-2; Nanjing Jiancheng Bioengineering Institute), malondialdehyde (MDA; cat. no. A003-1-1; Nanjing Jiancheng Bioengineering Institute), and ATP (cat. no. A095-1-1; Nanjing Jiancheng Bioengineering Institute) according to the manufacturer's instructions.

Immunofluorescence (IF) staining. Slides with cells were fixed with 4% neutral formaldehyde for 20 min at 4˚C. After washing with 1x PBS, the cell slides were treated with 0.1% Triton X-100 and 3% goat serum (cat. no. ZLI-9022; OriGene Technologies, Inc.) for 5 min at 4˚C. All antibodies were diluted using an antibody dilution buffer (cat. no. ZLI-9030; OriGene Technologies, Inc.) at a ratio of 1:200. The cells were then incubated with antibodies against ATP synthase F1 β subunit (ATP5B; cat. no. CL594-6660; ProteinTech Group, Inc.), activating transcription factor 6 (ATF6; cat. no. 66563-1-Ig; ProteinTech Group, Inc.), TSPO (cat. no. ab109497; Abcam) and LC3B (cat. no. ab51520; Abcam) overnight at 4˚C. Subsequently, the slides were incubated with chicken anti-rabbit IgG (H+L) cross-adsorbed secondary antibody (Alexa Fluor™ 488; cat. no. A21441; Invitrogen, Thermo Fisher Scientific, Inc.) or F(ab')2-goat anti-mouse IgG (H+L) cross-adsorbed secondary antibody (Alexa Fluor™ 546; cat. no. A11018; Invitrogen Thermo Fisher Scientific, Inc.) at room temperature for 1 h. Finally, the coverslip was sealed with DAPI Fluoromount-G™ (cat. no. 36308ES20, Shanghai Yeasen Biotechnology Co., Ltd.), and the cells were observed using a fluorescence microscope.

Co-immunoprecipitation (Co-IP). Co-IP was performed using a rProtein A/G Magnetic IP/Co-IP Kit (cat. no. AM001-01; ACE Biotechnology) according to the manufacturer's instructions. ATF6 (cat. no. 24169-1-AP; ProteinTech Group, Inc.), TSPO (cat. no. ab109497; Abcam), rabbit IgG control polyclonal antibody (cat. no. 30000-0-AP; ProteinTech Group, Inc.), and 20 μl magnetic beads each groups were mixed at 4˚C for 10 h. The mixture was then placed on a magnetic stand, and after separation, the supernatant was discarded. The magnetic beads were washed with 500 μl lysis buffer. After subjecting H9c2 cardiomyocytes to A/R, a lysis buffer was used to extract total protein. The protein concentration was determined using a BCA protein assay kit (cat. no. KGP902; Nanjing KeyGen Biotech Co., Ltd.). A portion of the extracted protein, approximately 100 μg, was used as the input group. Divide the remaining protein into groups of 400 μg, add them to EP tubes containing magnetic beads incubated with antibodies, and incubate them in a mixed spin at 4˚C for 6 h. The supernatant was then discarded, and the magnetic beads were washed twice with 500 μl lysis buffer. Finally, 5x loading buffer (cat. no. P0015; Beyotime Institute of Biotechnology) was diluted to 1x with lysis buffer, and the magnetic beads were heated in 1x loading buffer at 100˚C for 5 min. Western blotting was then performed for detection.

Reverse transcription-quantitative PCR (RT-qPCR). RT-qPCR analysis for TSPO gene expression: After specific treatments, samples were collected using Trizol reagent (cat. no. 10296010CN; Thermo Fisher Scientific, Inc.) to quantify the TSPO gene expression. The following primers were used for TSPO: Forward primer (5'-3'), CTGCCCGCTTGCTGTATC CTTAC; and the reverse primer (5'-3'), CGACCAGAGTTA TCACGCCATAC. GAPDH was used as an internal control: Forward primer (5'-3'), ACAGCA ACAGGGTGGTGGAC; and the reverse primer (5'-3'), TTTGAGGGTGCAGCGAAC TT. For the isolation of total RNA the RNA GeneJET RNA Purification kit (cat. no. K0731; Thermo Fisher Scientific, Inc.) was used, Dilute RNA to 200 ng/μl. And cDNA synthesis was

used cDNA Synthesis SuperMix (cat. no. 11141ES60; Shanghai Yeasen Biotechnology Co., Ltd.). Add 5 μl of diluted RNA, 2 μl of RNase free H2O, 2 μl of 5x gDNA Eraser buffer, and 1 μl of gDNA Eraser; Keep at 42˚C for 2 min to remove genomic DNA and then cool to 4˚C for cDNA synthesis; Then add 4 μl of RNA-free H2O, 4 μl of 5x PrimeScript Buffer 2, 1 μl of PrimeScript RT Enzyme Mix, and 1 μl of RT Primer Mix to the EP tube. Incubate at 37˚C for 15 min, followed by 85˚C for 5 sec, and finally cool to 4˚C for storage to proceed with cDNA amplification. cDNA amplification using SYBR Green Master Mix (cat. no. 11200ES08; Shanghai Yeasen Biotechnology Co., Ltd.). Dilute the above cDNA from 20 μl to 300 μl using RNase free H2O, take 9.2 μl cDNA, 10 μl Hieff UNICEF Universal Blue qPCR SYBR Green Master Mix, 0.4 μl Forward Primer (10 μM), 0.4 μl Reverse Primer (10 μM) into EP tubes, and wait for amplification. The quantitative PCR thermal cycling program for 40 cycles was: 1 cycle of enzyme activation at 95˚C for 15 min, denaturation at 95˚C for 30 sec, annealing at 60˚C for 30 sec and extension at 72˚C for 30 sec. Relative quantification was calculated using the $2^{-\Delta\Delta Ct}$ method (21).

Western blotting. H9c2 cardiomyocytes were lysed with RIPA buffer on ice, and the protein concentration was determined using a BCA protein assay kit (cat. no. KGP902; Nanjing KeyGen Biotech Co., Ltd.). Equal amounts of protein (20 μg per lane) were loaded using 8-12% SDS-PAGE and then transferred to a PVDF membrane. Membranes were blocked with 5% skimmed milk at room temperature for 1 h, then incubated with the following primary antibodies overnight at 4˚C: GAPDH (cat. no. HRP-60004; ProteinTech Group, Inc.), cleaved-caspase-3 (cat. no. 9661S; Cell Signaling Technology, Inc.), caspase-3 (cat. no. 66470-1-Ig; ProteinTech Group, Inc.), Bax (cat. no. 2772S; Cell Signaling Technology, Inc.), Bcl-2 (cat. no. 26593-1-AP; ProteinTech Group, Inc.), TSPO (cat. no. ab109497; Abcam), LC3B (cat. no. ab51520; Abcam), ATG5 (cat. no. 12994S; Cell Signaling Technology, Inc.), Beclin 1 (cat. no. 66665-1-Ig; ProteinTech Group, Inc.), P62 (23214S; ProteinTech Group, Inc.), PINK1 (cat. no. 23274-1-AP; ProteinTech Group, Inc.), Parkin (cat. no. 66674-1-Ig; ProteinTech Group, Inc.), Mfn2 (cat. no. 12186-1-AP; ProteinTech Group, Inc.), Drp1 (cat. no. 12957-1-AP; ProteinTech Group, Inc.), ATP5B (cat. no. 17247-1-AP; ProteinTech Group, Inc.), PI3K (cat. no. 4257S; Cell Signaling Technology, Inc.), phosphorylated (p)-PI3K (cat. no. 4228S; Cell Signaling Technology, Inc.), Akt (cat. no. 9272S, Cell Signaling Technology, Inc.), p-Akt (cat. no. 4060S; Cell Signaling Technology, Inc.), mTOR (cat. no. 2983S; Cell Signaling Technology, Inc.), p-mTOR (cat. no. 2971S; Cell Signaling Technology, Inc.), PKR-like ER kinase (PERK; cat. no. ab229912; Abcam), p-PERK (cat. no. 3179S; Cell Signaling Technology, Inc.), ATF6 (cat. no. 24169-1-AP; ProteinTech Group, Inc.) and inositol-requiring enzyme 1 (IRE1; cat. no. bs16696R, BIOSS). All primary antibodies were diluted using an antibody dilution buffer (cat. no. P0023A-500ml; Beyotime Institute of Biotechnology) at a ratio of 1:1,000. After incubation with the primary antibody, the membrane was washed three times with Tris-buffered saline and 0.1% Tween 20 (cat. no. 1247ML500; Biofroxx, Inc.) and then according to the primary antibody species incubated with rabbit secondary antibodies (cat. no. 7074P2; Cell Signaling Technology, Inc.) or mouse secondary antibodies (cat. no. 7076S; Cell Signaling Technology, Inc.) at room temperature for 1 h. All secondary antibodies were diluted using an antibody dilution buffer (cat. no. P0023A-500ml; Beyotime Institute of Biotechnology) at a ratio of 1:5,000. Signals were visualized using Immobilon western chemiluminescence HRP substrate (cat. no. WBKLS0500, MilliporeSigma) and imaged using a ChemiScope (Clinx Science Instruments). Densitometry analysis was performed using chemical analysis software (version 2017.12.6.0; Clinx Science Instruments).

Statistical analysis. Data are presented as the mean ± the standard error of the mean. The distribution of data was assessed using a Shapiro-Wilk test. For comparisons between two groups, a independent sample t-test was used. Comparisons between multiple groups were assessed using a one-way ANOVA followed by a post hoc Tukey's test. All statistical analysis was performed using GraphPad Prism version 9.0 (GraphPad Software, Inc.; Dotmatics). $P<0.05$ was considered to indicate a statistically significant difference.

Results

TSPO knockdown alleviates myocardial apoptosis and damage following A/R stimulation. To investigate the impact of TSPO on myocardial I/R, an A/R model was established using the H9c2 myocardial cells. The western blotting results showed a significant increase in the protein expression levels of TSPO following anoxia. Knockdown of *TSPO* using siRNA led to a significant reduction in TSPO levels following A/R stimulation compared with the control group (Fig. 1A and B). Moreover, the results showed that the levels of proapoptotic molecules Bax and cleaved-caspase-3/caspase-3 were significantly increased in H9c2 si-NC-transfected cardiomyocytes following A/R stimulation compared with the si-NC-transfected control cells; subsequently, the levels of proapoptotic molecules Bax and cleaved-caspase-3/caspase-3 were significantly decreased following *TSPO* knockdown. By contrast, in H9c2 si-TSPO-transfected cardiomyocytes following A/R stimulation compared with si-NC-transfected cardiomyocytes following A/R stimulation the show that *TSPO* knockdown resulted in a slight upregulation of the antiapoptotic molecule Bcl-2 (Fig. 1A and B). Consistently, FACS-based apoptosis analysis revealed that the knockdown of *TSPO* decreased the levels of apoptosis induced by A/R (Fig. 1C and D). Furthermore, LDH levels were assessed as a marker of cell damage and quantified using an enzymatic activity assay. The results showed that cell damage was significantly increased following A/R stimulation and was reduced following *TSPO* knockdown (Fig. 1E). In agreement with the aforementioned observations, CCK-8 analysis revealed a significant decrease in myocardial cell activity in response to A/R stimulation, but this decrease was attenuated following *TSPO* knockdown (Fig. 1F). The aforementioned results suggest that inhibiting TSPO may be a potential strategy for mitigating myocardial I/R injury by decreasing cell apoptosis and damage.

Targeting TSPO improves mitochondrial dysfunction in myocardial cells following A/R stimulation. Considering the cellular location and previously reported functions of TSPO,

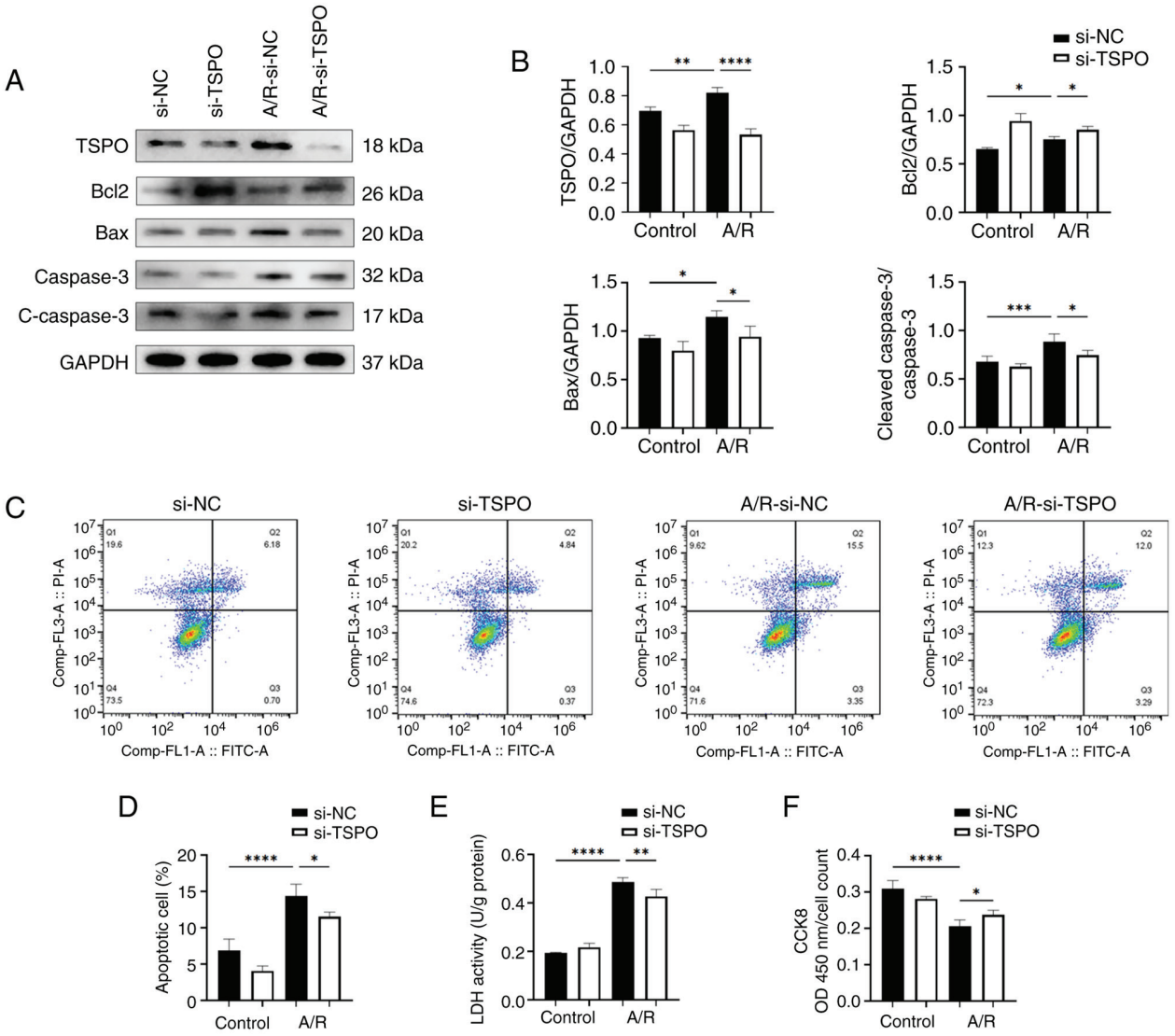

Figure 1. Targeting TSPO alleviates myocardial apoptosis and damage in an *in vitro* A/R model. (A and B) Western blotting and densitometry analysis of TSPO, Bcl2, Bax and cleaved-caspase-3/caspase-3 expression levels in si-NC and si-TSPO H9c2 cells with or without A/R stimulation. (C) Representative flow cytometry results showing the apoptosis of H9c2 cells determined using Annexin V-FITC/PI double-staining assay. (D) Quantification of the percentage of late apoptotic H9c2 cells. (E) Cell damage was measured using an LDH assay. (F) Cell viability was measured using a Cell Counting Kit-8 assay. n=4 per group. *P<0.05, **P<0.01, ***P<0.001, ****P<0.0001. TSPO, translocator protein; A/R, anoxia/reoxygenation; si, small interfering; NC, negative control; LDH, lactate dehydrogenase; FITC, fluorescein isothiocyanate; PI, propidium iodide.

the interplay between TSPO and mitochondrial dysfunction was next explored. A JC-1 assay kit was used to detect the mitochondrial membrane potential, as indicated by the red/green fluorescence ratio. The results revealed a significant decrease in the membrane potential of myocardial cells following A/R stimulation, which was significantly attenuated following *TSPO* knockdown (Fig. 2A and B). Notably, ATP production can reflect mitochondrial function. The results further showed that after *TSPO* knockdown, ATP production was significantly increased (Fig. 2C). Consistent with these findings, ATP5B, a crucial subunit of mitochondrial ATP synthase, was upregulated following the knockdown of *TSPO* and A/R stimulation (Figs. 2D, E and S2).

Subsequently, the effect of TSPO on the oxidative stress levels of myocardial cells following A/R stimulation. Notably, a significant increase in ROS and mtROS levels was observed in si-NC-transfected myocardial cells following A/R stimulation, and these changes were significantly decreased following *TSPO* knockdown (Fig. 2F and G). Moreover, the levels of SOD, a marker of antioxidant enzymes, significantly decreased in si-NC-transfected myocardial cells in response to A/R stimulation and increased after *TSPO* knockdown (Fig. 2H). By contrast, the levels of MDA, a marker of cell membrane lipid oxidation, were significantly increased in si-NC-transfected myocardial cells following A/R stimulation and decreased following *TSPO* knockdown (Fig. 2I). These results indicate that targeting TSPO could efficiently improve mitochondrial function and concomitantly alleviate oxidative stress.

ER stress and mitophagy may mediate TSPO-driven mitochondrial dysfunction following A/R stimulation. To investigate how *TSPO* knockdown protected against mitochondrial dysfunction

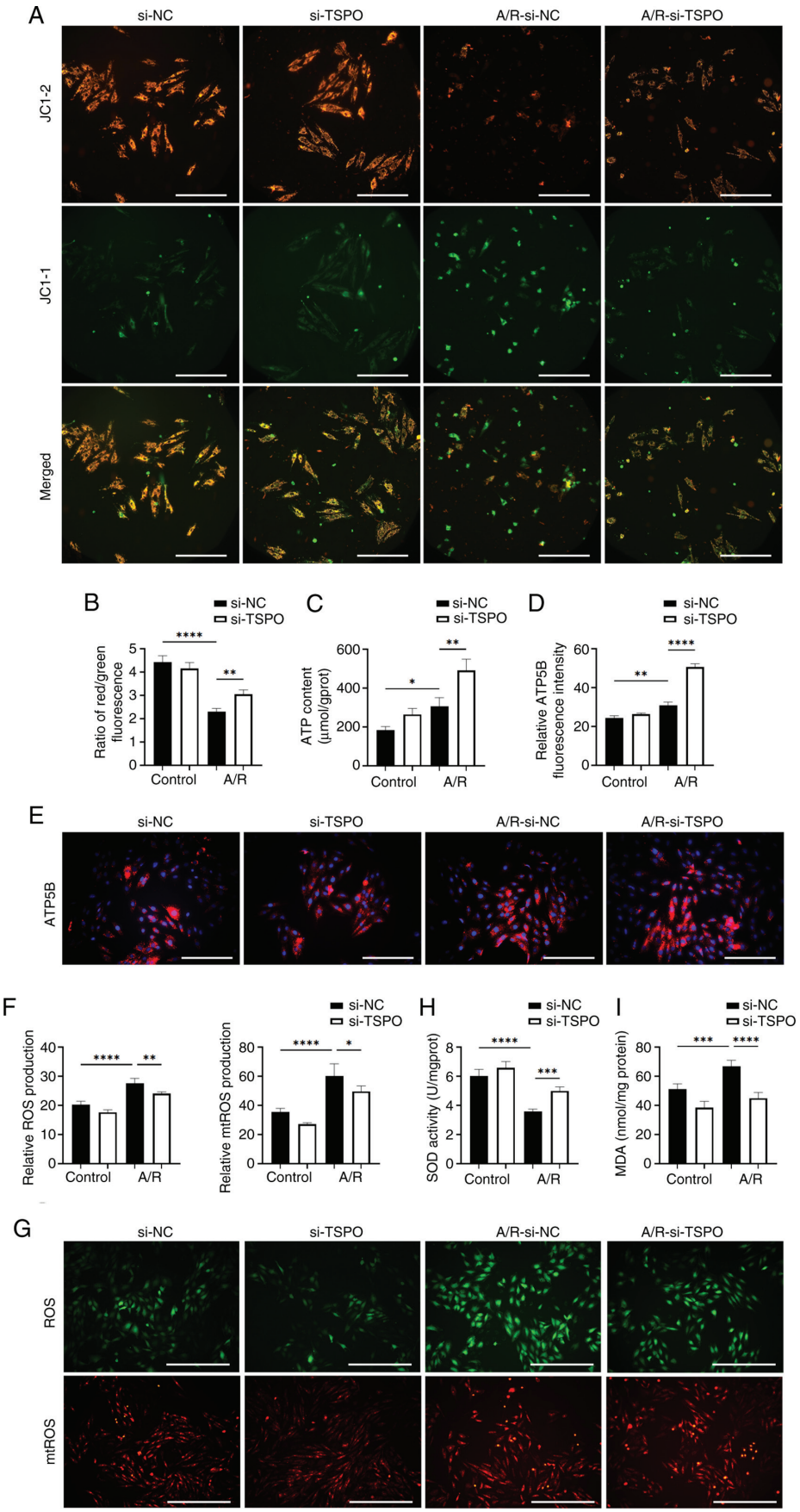

Figure 2. *TSPO* knockdown reduces mitochondrial dysfunction in myocardial cells following A/R stimulation. (A and B) Representative fluorescence images and quantitative analysis of JC-1 staining in si-NC and si-TSPO H9c2 cells with or without A/R stimulation. Scale bar, 20 μm. (C) Quantitative analysis of the ATP content in the different groups. (D and E) Representative fluorescence images and quantitative analysis of ATP5B expression. Scale bar, 20 μm. (F) Quantitative analysis and (G) representative images and of ROS and mtROS staining. Scale bar, 50 μm. (H) Quantitative analysis of SOD activity and (I) MDA levels. *P<0.05, **P<0.01, ***P<0.001, ****P<0.0001. TSPO, translocator protein; A/R, anoxia/reoxygenation; si, small interfering; NC, negative control; ROS, reactive oxygen species; mtROS, mitochondrial ROS; SOD, superoxide dismutase; MDA, malondialdehyde; ATP5B, ATP synthase F1 β subunit.

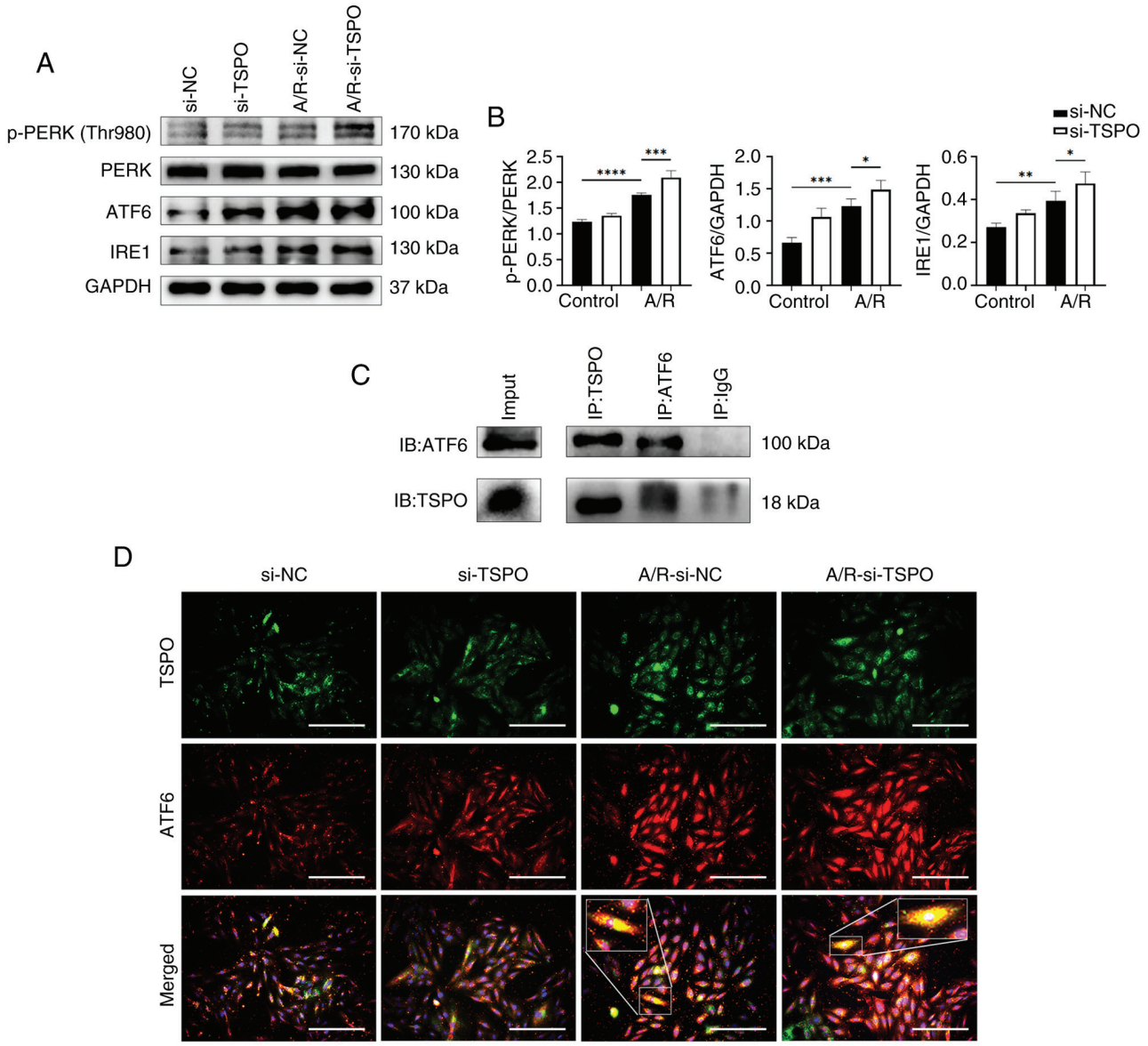

Figure 3. TSPO interacts with ATF6 and promotes endoplasmic reticulum stress following A/R stimulation. (A) Western blotting and (B) densitometry analysis of p-PERK, PERK, ATF6 and IRE1 protein expression levels in si-NC and si-TSPO H9c2 cells with or without A/R stimulation. (C) Co-immunoprecipitation of TSPO and ATF6. (D) Multiplex immunocytochemistry analysis of TSPO and ATF6. 4 times magnification for the zoomed in box. Scale bar, 20 μm. *P<0.05, **P<0.01, ***P<0.001, ****P<0.0001. TSPO, translocator protein; A/R, anoxia/reoxygenation; si, small interfering; NC, negative control. IRE1, inositol-requiring enzyme 1.

induced by A/R stimulation, the impact of TSPO on ER stress was explored. ER stress is closely associated with mitochondrial dysfunction by transferring stress signals from the ER to the mitochondria (22). Western blotting confirmed that A/R stimulation resulted in a significant increase in the expression of key markers (p-PERK/PERK, ATF6 and IRE1) involved in the adaptive unfolded protein response (UPR), accompanied by downstream signaling during ER stress (23). However, *TSPO* knockdown further increased the expression of the aforementioned markers compared with the si-NC A/R group (Fig. 3A and B). Subsequently, Co-IP results show that there is a protein interaction between TSPO and ATF6 (Fig. 3C). In addition, immunofluorescence co-staining showed an increase in ATF6 expression in the nucleus following A/R stimulation. The localization of ATF6 in the cytoplasm overlapped with TSPO (Fig. 3D). These results indicate that TSPO may play a role in ER stress by interacting with ATF6 during myocardial I/R injury.

ER stress is also a potent trigger for autophagy, which typically serves an adaptive protective function during myocardial I/R injury (24). Paradoxically, the results showed that *TSPO* knockdown reduced the expression of autophagy-related markers following A/R stimulation compared with si-NC A/R cells (Fig. 4A-C). Notably, the PI3K-Akt-mTOR pathway participates in inhibiting the activation of autophagy (25). In the present study, following *TSPO* knockdown, the ratios of p-PI3K/PI3K, p-Akt/Akt and p-mTOR/mTOR were significantly increased compared with si-NC A/R cells (Fig. 4D and E). These results suggest that targeting TSPO may inhibit myocardial cell autophagy by promoting the activation of the PI3K-Akt-mTOR signaling pathway.

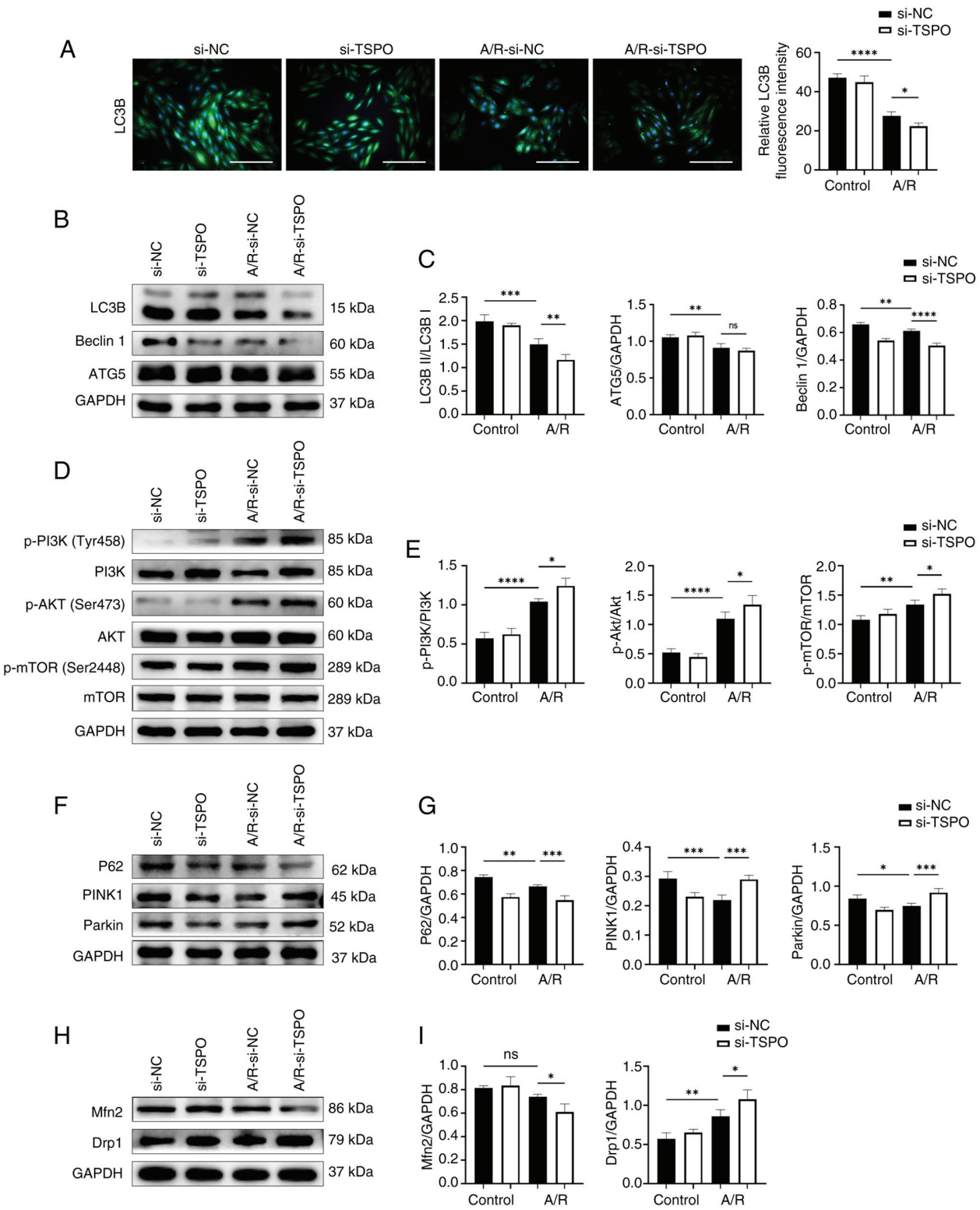

Figure 4. TSPO regulates autophagy and mitophagy via related pathways following A/R stimulation. (A) Representative fluorescence images and quantitative analysis of LC3B expression. Scale bar, 20 μm. (B) Western blotting and (C) densitometry analysis of LC3B, Beclin1 and ATG5 expression levels in si-NC and si-TSPO H9c2 cells with or without A/R stimulation. (D) Western blotting and (E) densitometry analysis of p-PI3K, PI3K, p-Akt, Akt, p-mTOR and mTOR expression levels. (F) Western blotting and (G) densitometry analysis of P62, PINK1 and Parkin expression levels. (H) Western blotting and (I) densitometry analysis of Mfn2 and Drp1 protein expression levels. *P<0.05, **P<0.01, ***P<0.001, ****P<0.0001. TSPO, translocator protein; A/R, anoxia/reoxygenation; si, small interfering; NC, negative control; p-, phosporylated.

Subsequently, the expression of mitophagy-related proteins (P62, PINK1 and Parkin) were assessed. A/R stimulation induced a significant decrease in mitophagy-related markers, while TSPO knockdown following A/R treatment upregulated the levels of these mitophagy markers, as indicated by further decreases in P62 expression and increases in Parkin and PINK1 expression compared with si-NC A/R controls (Fig. 4F and G). Furthermore, *TSPO* knockdown resulted in

a significant decrease in the expression of the mitochondrial fusion protein Mfn2 following A/R stimulation compared with si-NC A/R controls. However, the protein levels of Drp1, a typical marker of mitochondrial fission, significantly increased following *TSPO* knockdown compared with si-NC A/R controls (Fig. 4H and I). These results suggest that inhibiting TSPO may decrease the fusion of damaged and healthy mitochondria in myocardial cells, promote mitochondrial fission, and facilitate the clearance of damaged mitochondria through the Parkin/PINK1-mediated mitophagy pathway following A/R stimulation. This process may help alleviate mitochondrial dysfunction during myocardial I/R injury.

Discussion

Myocardial I/R injury is a significant complication that occurs following a myocardial infarction (26). Despite significant research efforts to identify therapeutic targets to address this condition, advancements in the clinical management of this disease have proven to be challenging. In the present study, it was demonstrated that TSPO was significantly induced following A/R injury. Knockdown of *TSPO* led to reduced apoptosis and a simultaneous reduction in mitochondrial dysfunction following A/R injury. Furthermore, it was found that ER stress persisted in cells subjected to A/R and was intensified further in the *TSPO* knockdown cells. The interaction between TSPO and the ER stress-related protein ATF6 suggested that ER stress may play a role in mediating TSPO-driven mitochondrial dysfunction following A/R stimulation, highlighting the need for further investigations. Taken together, these results suggest that targeting TSPO may be a promising strategy for alleviating myocardial I/R injury. TSPO may thus function as a potential mediator of the relationship between ER stress and mitochondrial dysfunction.

Emerging evidence has confirmed that apoptosis in cardiomyocytes may result from mitochondrial injury, autophagy, oxidative stress and ER stress (27). However, the underlying link between the aforementioned cellular events remains elusive. Since TSPO is an OMM protein expressed in the heart (11), and the TSPO ligand 4'-chlorodiazepam has been shown to reduce infarct size and enhance mitochondrial function post-ischemia-reperfusion (28), a focus was placed on assessing the impact of TSPO on myocardial I/R injury. The results of the present study revealed that following A/R stimulation, TSPO expression significantly increased, as did cardiomyocyte apoptosis, which was notably reduced following *TSPO* knockdown.

The role of mtROS production and related pathways in myocardial I/R injury has been extensively studied (7). Myocardial ischemia hinders the mitochondrial ETC due to oxygen deprivation, leading to excessive ROS production and consequent cellular damage during reperfusion, ultimately resulting in apoptosis (6). However, the exact mechanism of myocardial I/R injury has not been fully determined, and relevant clinical trials have proven to be ineffective (5). These findings support previous research indicating that *TSPO* knockdown alleviates oxidative stress and consequent apoptosis in cardiomyocytes during A/R.

To further clarify the underlying mechanisms of TSPO in myocardial I/R injury, its regulatory effect on mitochondrial function was investigated. Liu *et al* (14) demonstrated the involvement of TSPO in the regulation of ATP synthesis. The authors noted that overexpression of *TSPO* in Jurkat cells increases mitochondrial ATP production and cellular excitability. Paradoxically, Gatliff *et al* (15) reported that TSPO overexpression, in conjunction with its interaction with voltage-dependent anion channel 1, enhances mtROS synthesis while inhibiting mitophagy and ATP production in canine mammary epithelial cells. In the present study, it was confirmed that targeting TSPO facilitated ATP synthesis in cardiomyocytes following A/R stimulation. This effect was likely attributed to reduced ROS production and efficient clearance of damaged mitochondria (29). Moreover, the decrease in the mitochondrial membrane potential was mitigated following *TSPO* knockdown. Thus, TSPO may participate in myocardial I/R injury by regulating energy synthesis and ROS generation.

Mitochondria and the ER play a fundamental role in controlling cellular physiology and regulating diverse signal transduction pathways. The mitochondria-associated membranes (MAMs) represent the first discovered connection between these two organelles, forming specialized lipid raft-like structures (30). MAMs possess distinct structures and serve as platforms for various signal transduction functions, including lipid synthesis, transport and calcium transfer from the ER to the mitochondria (31). Consequently, they regulate crucial signaling pathways and maintain cellular homeostasis. During myocardial I/R, an extensive UPR occurs (32). ER stress, triggered by the accumulation of unfolded or misfolded proteins in the ER, activates various cellular processes, including oxidative stress leading to mitochondrial dysfunction (33). Evidence suggests that myocardial cells experience increased ER stress following I/R, with ATF6 knockdown exacerbating heart damage and functional decline post-I/R (34). The present study showed that targeting TSPO triggered ER stress in cardiomyocytes following A/R stimulation, and Co-IP analysis revealed an interaction between TSPO and ATF6. Notably, ER stress-induced autophagy is a compensatory response to cellular stress; however, prolonged or severe ER stress can precipitate cell death (35). The activation of the UPR can lead to apoptosis, but it can also trigger protective mechanisms, such as autophagy (36). According to Vanhoutte *et al* (37), the Thbs1-mediated PERK-eIF2α-ATF4 signaling pathway plays a crucial role in inducing autophagy and regulating cardiomyocyte size in the stressed heart. Margariti *et al* (38) identified the IRE1α-XBP1-S axis, which promotes the conversion of LC3 I to LC3 II in endothelial cells, thereby promoting autophagy. Dang *et al* (39) found that under ER stress, ATF6 enhances autophagy and connects UPR-associated pathways to maintain ER homeostasis. Overexpression of activated ATF6 also rescues defects in autophagy regulation (39). These studies substantiate the role of ER stress in modulating autophagy, in agreement with the findings of the present study. Autophagy is suppressed in the myocardium during I/R (40). This process maintains cardiomyocyte function by removing damaged organelles and proteins. Appropriate levels of autophagy are essential for myocardial recovery (41); however, excessive autophagy can lead to cardiomyocyte death and reduced myocardial function. In the present study, following A/R, autophagy in H9c2 cardiomyocytes was significantly decreased, and autophagy

further decreased following TSPO knockdown. Concurrently, the PI3K-Akt-mTOR pathway was notably activated following A/R stimulation and further enhanced following TSPO knockdown, suggesting that TSPO may modulate autophagy via this pathway.

In prior studies, the role of DRP1 promotes the production of ROS (42). During I/R injury, both Fis1 and DRP1 are upregulated in neonatal and adult cardiomyocytes (43,44). In this scenario, upstream signaling events promote the activation of DRP1, which then interacts with Fis1 at the OMM (45). This interaction leads to an excessive accumulation of fragmented and dysfunctional mitochondria, resulting in a redox imbalance (46). Fis1 also binds to mitochondrial fusion proteins (MFN1, MFN2 and OPA1) and inhibits their GTPase activity, consequently impeding mitochondrial fusion in mammalian cells (47). The expression of MFN2 and DRP1 shows a negative correlation and jointly contributes to the regulation of mitochondrial size (48). In the present study, the inconsistency in the expression of ROS and DRP1 may be attributed to the function of TSPO. The interaction between TSPO and VDAC1 can influence ROS production (15,16). Previous studies have shown that TSPO knockdown significantly reduces ROS expression (15,16). Hence, it is plausible to suggest that TSPO knockdown could potentially inhibit the DRP1-mediated increase in ROS.

Notably, in addition to autophagy, mitophagy, which is crucial for removing damaged mitochondria and maintaining cellular homeostasis (49), is inversely associated with TSPO levels (17). In the present study, it was observed that A/R treatment significantly reduced mitophagy. Following *TSPO* knockdown, the extent of mitophagy significantly increased. In general, impaired mitochondrial function hampers ATP synthesis (50). However, the present study revealed that cardiomyocytes with reduced TSPO expression produced more ATP following A/R stimulation. This could be attributed to enhanced clearance of damaged mitochondria and restoration of mitochondrial function (51). Additionally, the activation of ER stress may assist in the elimination of accumulated unfolded proteins, requiring a significant amount of ATP (52). These findings suggest that mitochondrial function is partially restored in cardiomyocytes following A/R stimulation with *TSPO* expression knocked down. Based on these observations, it is postulated that *TSPO* knockdown would mitigate damage in cardiomyocytes following A/R stimulation, potentially by triggering persistent ER stress and concomitant induction of mitophagy. However, the precise mechanisms of TSPO warrant further investigation.

It is necessary to acknowledge the limitations of the present work. This study only used an *in vitro* model. Although this provides mechanistic insights, further validation of the reliability and general applicability of the research results using animal models and clinical samples is required. Furthermore, other unexplored signaling pathways and mechanisms related to TSPO in myocardial I/R injury may require further investigation for clarification in future studies.

In conclusion, the role of TSPO was investigated in an *in vitro* model of A/R injury using H9c2 cardiomyocytes. The results establish a potential mechanistic association between ER stress and TSPO-induced mitochondrial dysfunction in the process of myocardial I/R injury. Taken together, these results suggest that targeting TSPO may be a potential strategy for alleviating myocardial I/R injury in patients with IHD.

Acknowledgements

The authors would like to thank Dr Xu Duo, Department of Oncology, The First Affiliated Hospital of Nanjing Medical University, Nanjing, China, for her assistance in performing experiments.

Funding

This study was supported by The Nanjing Scientific Research Project for Outstanding Overseas Students (grant no. #2021) and The Key Medical Research Project from the Jiangsu Provincial Health Commission (grant no. K2023039).

Availability of data and materials

The data generated in the present study may be requested from the corresponding author.

Authors' contributions

CW, ZQ and SL conceived and designed the experiments. CW, YJ, SL, ZQ, WC, YX, GC, QZ, HJ, YL, YY and XC carried out the experiments. CW and YJ cultured the cells. ZQ and SL treated the cells. GC and YL designed the primers and performed the reverse transcription-quantitative PCR. YJ, WC and YX performed the flow cytometric analysis. CW, SL and ZQ performed Co-IP experiment. QZ and HJ performed the mitochondrial membrane potential, ROS and mtROS assay. CW and YJ performed LHD and CCK8 assay. XC and YY performed MDA and SOD assays. CW, YJ, SL, WC, YX, QZ, YY and XC performed the western blot analysis. QL and RZ quantified and analyzed the raw data. ZQ and SL confirmed the authenticity of all raw data. CW drafted the original manuscript. All authors have read and approved the final manuscript.

Ethics approval and consent to participate

Not applicable.

Patient consent for publication

Not applicable.

Competing interests

The authors declare that they have no competing interests.

References

1. Roth GA, Mensah GA, Johnson CO, Addolorato G, Ammirati E, Baddour LM, Barengo NC, Beaton AZ, Benjamin EJ, Benziger CP, *et al*: Global burden of cardiovascular diseases and risk factors, 1990-2019: Update from the GBD 2019 study. J Am Coll Cardiol 76: 2982-3021, 2020.
2. Doenst T, Thiele H, Haasenritter J, Wahlers T, Massberg S and Haverich A: The treatment of coronary artery disease. Dtsch Arztebl Int 119: 716-723, 2022.
3. Bhatt DL, Lopes RD and Harrington RA: Diagnosis and treatment of acute coronary syndromes: A review. JAMA 327: 662-675, 2022.

4. Martí-Pàmies Í, Thoonen R, Morley M, Graves L, Tamez J, Caplan A, McDaid K, Yao V, Hindle A, Gerszten RE, *et al*: Brown adipose tissue and BMP3b decrease injury in cardiac ischemia-reperfusion. Circ Res 133: 353-365, 2023.
5. Heusch G: Myocardial ischaemia-reperfusion injury and cardioprotection in perspective. Nat Rev Cardiol 17: 773-789, 2020.
6. Jiang L, Yin X, Chen YH, Chen Y, Jiang W, Zheng H, Huang FQ, Liu B, Zhou W, Qi LW and Li J: Proteomic analysis reveals ginsenoside Rb1 attenuates myocardial ischemia/reperfusion injury through inhibiting ROS production from mitochondrial complex I. Theranostics 11: 1703-1720, 2021.
7. Xiang Q, Yi X, Zhu XH, Wei X and Jiang DS: Regulated cell death in myocardial ischemia-reperfusion injury. Trends Endocrinol Metab 35: 219-234, 2024.
8. Chen CL, Zhang L, Jin Z, Kasumov T and Chen YR: Mitochondrial redox regulation and myocardial ischemia-reperfusion injury. Am J Physiol Cell Physiol 322: C12-C23, 2022.
9. Papadopoulos V, Baraldi M, Guilarte TR, Knudsen TB, Lacapère JJ, Lindemann P, Norenberg MD, Nutt D, Weizman A, Zhang MR and Gavish M: Translocator protein (18kDa): New nomenclature for the peripheral-type benzodiazepine receptor based on its structure and molecular function. Trends Pharmacol Sci 27: 402-409, 2006.
10. Banati RB, Middleton RJ, Chan R, Hatty CR, Kam WWY, Quin C, Graeber MB, Parmar A, Zahra D, Callaghan P, *et al*: Positron emission tomography and functional characterization of a complete PBR/TSPO knockout. Nat Commun 5: 5452, 2014.
11. Selvaraj V and Stocco DM: The changing landscape in translocator protein (TSPO) function. Trends Endocrinol Metab 26: 341-348, 2015.
12. Braestrup C, Albrechtsen R and Squires RF: High densities of benzodiazepine receptors in human cortical areas. Nature 269: 702-704, 1977.
13. Farhan F, Almarhoun M, Wong A, Findlay AS, Bartholomew C, Williams MTS, Hurd TW and Shu X: Deletion of TSPO causes dysregulation of cholesterol metabolism in mouse retina. Cells 10: 3066, 2021.
14. Liu GJ, Middleton RJ, Kam WWY, Chin DY, Hatty CR, Chan RHC and Banati RB: Functional gains in energy and cell metabolism after TSPO gene insertion. Cell Cycle 16: 436-447, 2017.
15. Gatliff J, East D, Crosby J, Abeti R, Harvey R, Craigen W, Parker P and Campanella M: TSPO interacts with VDAC1 and triggers a ROS-mediated inhibition of mitochondrial quality control. Autophagy 10: 2279-2296, 2014.
16. Meng Y, Tian M, Yin S, Lai S, Zhou Y, Chen J, He M and Liao Z: Downregulation of TSPO expression inhibits oxidative stress and maintains mitochondrial homeostasis in cardiomyocytes subjected to anoxia/reoxygenation injury. Biomed Pharmacother 121: 109588, 2020.
17. Scaini G, Barichello T, Fries GR, Kennon EA, Andrews T, Nix BR, Zunta-Soares G, Valvassori SS, Soares JC and Quevedo J: TSPO upregulation in bipolar disorder and concomitant downregulation of mitophagic proteins and NLRP3 inflammasome activation. Neuropsychopharmacology 44: 1291-1299, 2019.
18. Ma XH, Liu JH, Liu CY, Sun WY, Duan WJ, Wang G, Kurihara H, He RR, Li YF, Chen Y and Shang H: ALOX15-launched PUFA-phospholipids peroxidation increases the susceptibility of ferroptosis in ischemia-induced myocardial damage. Signal Transduct Target Ther 7: 288, 2022.
19. Pooja S, Pushpanathan M, Gunasekaran P and Rajendhran J: Endocytosis-mediated invasion and pathogenicity of streptococcus agalactiae in rat cardiomyocyte (H9C2). PLoS One 10: e0139733, 2015.
20. Tong Z, Xie Y, He M, Ma W, Zhou Y, Lai S, Meng Y and Liao Z: VDAC1 deacetylation is involved in the protective effects of resveratrol against mitochondria-mediated apoptosis in cardiomyocytes subjected to anoxia/reoxygenation injury. Biomed Pharmacother 95: 77-83, 2017.
21. Livak KJ and Schmittgen TD: Analysis of relative gene expression data using real-time quantitative PCR and the 2(-Delta Delta C(T)) method. Methods 25: 402-408, 2001.
22. Martucciello S, Masullo M, Cerulli A and Piacente S: Natural products targeting ER stress, and the functional link to mitochondria. Int J Mol Sci 21: 1905, 2020.
23. Salvagno C, Mandula JK, Rodriguez PC and Cubillos-Ruiz JR: Decoding endoplasmic reticulum stress signals in cancer cells and antitumor immunity. Trends Cancer 8: 930-943, 2022.
24. Wang CC, Li Y, Qian XQ, Zhao H, Wang D, Zuo GX and Wang K: Empagliflozin alleviates myocardial I/R injury and cardiomyocyte apoptosis via inhibiting ER stress-induced autophagy and the PERK/ATF4/Beclin1 pathway. J Drug Target 30: 858-872, 2022.
25. Ba L, Gao J, Chen Y, Qi H, Dong C, Pan H, Zhang Q, Shi P, Song C, Guan X, *et al*: Allicin attenuates pathological cardiac hypertrophy by inhibiting autophagy via activation of PI3K/Akt/mTOR and MAPK/ERK/mTOR signaling pathways. Phytomedicine 58: 152765, 2019.
26. Rizwan H, Pal S, Sabnam S and Pal A: High glucose augments ROS generation regulates mitochondrial dysfunction and apoptosis via stress signalling cascades in keratinocytes. Life Sci 241: 117148, 2020.
27. Wang J and Zhou H: Mitochondrial quality control mechanisms as molecular targets in cardiac ischemia-reperfusion injury. Acta Pharm Sin B 10: 1866-1879, 2020.
28. Paradis S, Leoni V, Caccia C, Berdeaux A and Morin D: Cardioprotection by the TSPO ligand 4'-chlorodiazepam is associated with inhibition of mitochondrial accumulation of cholesterol at reperfusion. Cardiovasc Res 98: 420-427, 2013.
29. Livingston MJ, Wang J, Zhou J, Wu G, Ganley IG, Hill JA, Yin XM and Dong Z: Clearance of damaged mitochondria via mitophagy is important to the protective effect of ischemic preconditioning in kidneys. Autophagy 15: 2142-2162, 2019.
30. Wang N, Wang C, Zhao H, He Y, Lan B, Sun L and Gao Y: The MAMs structure and its role in cell death. Cells 10: 657, 2021.
31. Pinton P: Mitochondria-associated membranes (MAMs) and pathologies. Cell Death Dis 9: 413, 2018.
32. Glembotski CC, Rosarda JD and Wiseman RL: Proteostasis and beyond: ATF6 in ischemic disease. Trends Mol Med 25: 538-550, 2019.
33. Senft D and Ronai ZA: UPR, autophagy, and mitochondria crosstalk underlies the ER stress response. Trends Biochem Sci 40: 141-148, 2015.
34. Jin JK, Blackwood EA, Azizi K, Thuerauf DJ, Fahem AG, Hofmann C, Kaufman RJ, Doroudgar S and Glembotski CC: ATF6 decreases myocardial ischemia/reperfusion damage and links ER stress and oxidative stress signaling pathways in the heart. Circ Res 120: 862-875, 2017.
35. Zhang J, Guo J, Yang N, Huang Y, Hu T and Rao C: Endoplasmic reticulum stress-mediated cell death in liver injury. Cell Death Dis 13: 1051, 2022.
36. Bhardwaj M, Leli NM, Koumenis C and Amaravadi RK: Regulation of autophagy by canonical and non-canonical ER stress responses. Semin Cancer Biol 66: 116-128, 2020.
37. Vanhoutte D, Schips TG, Vo A, Grimes KM, Baldwin TA, Brody MJ, Accornero F, Sargent MA and Molkentin JD: Thbs1 induces lethal cardiac atrophy through PERK-ATF4 regulated autophagy. Nat Commun 12: 3928, 2021.
38. Margariti A, Li H, Chen T, Martin D, Vizcay-Barrena G, Alam S, Karamariti E, Xiao Q, Zampetaki A, Zhang Z, *et al*: XBP1 mRNA splicing triggers an autophagic response in endothelial cells through BECLIN-1 transcriptional activation. J Biol Chem 288: 859-872, 2013.
39. Dang TT, Kim MJ, Lee YY, Le HT, Kim KH, Nam S, Hyun SH, Kim HL, Chung SW, Chung HT, *et al*: Phosphorylation of EIF2S1 (eukaryotic translation initiation factor 2 subunit alpha) is indispensable for nuclear translocation of TFEB and TFE3 during ER stress. Autophagy 19: 2111-2142, 2023.
40. Gu S, Tan J, Li Q, Liu S, Ma J, Zheng Y, Liu J, Bi W, Sha P, Li X, *et al*: Downregulation of LAPTM4B contributes to the impairment of the autophagic flux via unopposed activation of mTORC1 signaling during myocardial ischemia/reperfusion injury. Circ Res 127: e148-e165, 2020.
41. Del Re DP, Amgalan D, Linkermann A, Liu Q and Kitsis RN: Fundamental mechanisms of regulated cell death and implications for heart disease. Physiol Rev 99: 1765-1817, 2019.
42. Zeng X, Zhang YD, Ma RY, Chen YJ, Xiang XM, Hou DY, Li XH, Huang H, Li T and Duan CY: Activated Drp1 regulates p62-mediated autophagic flux and aggravates inflammation in cerebral ischemia-reperfusion via the ROS-RIP1/RIP3-exosome axis. Mil Med Res 9: 25, 2022.
43. Hom J, Yu T, Yoon Y, Porter G and Sheu SS: Regulation of mitochondrial fission by intracellular Ca2+ in rat ventricular myocytes. Biochim Biophys Acta 1797: 913-921, 2010.
44. Zhou H, Zhu P, Wang J, Zhu H, Ren J and Chen Y: Pathogenesis of cardiac ischemia reperfusion injury is associated with CK2α-disturbed mitochondrial homeostasis via suppression of FUNDC1-related mitophagy. Cell Death Differ 25: 1080-1093, 2018.

45. Yu Y, Peng XD, Qian XJ, Zhang KM, Huang X, Chen YH, Li YT, Feng GK, Zhang HL, Xu XL, *et al*: Fis1 phosphorylation by Met promotes mitochondrial fission and hepatocellular carcinoma metastasis. Signal Transduct Target Ther 6: 401, 2021.
46. Disatnik MH, Ferreira JCB, Campos JC, Gomes KS, Dourado PMM, Qi X and Mochly-Rosen D: Acute inhibition of excessive mitochondrial fission after myocardial infarction prevents long-term cardiac dysfunction. J Am Heart Assoc 2: e000461, 2013.
47. Yu R, Jin SB, Lendahl U, Nistér M and Zhao J: Human Fis1 regulates mitochondrial dynamics through inhibition of the fusion machinery. EMBO J 38: e99748, 2019.
48. Ziviani E, Tao RN and Whitworth AJ: Drosophila parkin requires PINK1 for mitochondrial translocation and ubiquitinates mitofusin. Proc Natl Acad Sci USA 107: 5018-5023, 2010.
49. Lu Y, Li Z, Zhang S, Zhang T, Liu Y and Zhang L: Cellular mitophagy: Mechanism, roles in diseases and small molecule pharmacological regulation. Theranostics 13: 736-766, 2023.
50. Tanno S, Yamamoto K, Kurata Y, Adachi M, Inoue Y, Otani N, Mishima M, Yamamoto Y, Kuwabara M, Ogino K, *et al*: Protective effects of topiroxostat on an ischemia-reperfusion model of rat hearts. Circ J 82: 1101-1111, 2018.
51. Wu D, Wang Y, Hu J, Xu Y, Gong D, Wu P, Dong J, He B, Qian H and Wang G: Rab26 promotes macrophage phagocytosis through regulation of MFN2 trafficking to mitochondria. FEBS J 290: 4023-4039, 2023.
52. Yong J, Bischof H, Burgstaller S, Siirin M, Murphy A, Malli R and Kaufman RJ: Mitochondria supply ATP to the ER through a mechanism antagonized by cytosolic Ca^2. Elife 8: e49682, 2019.